A MULTICOMPONENT SELF-SIMILAR CHARACTERIZATION OF RAINFALL FLUCTUATIONS*

PRAVEEN KUMAR† AND EFI FOUFOULA-GEORGIOU‡

Abstract. Issues of scaling characteristics in spatial rainfall have attracted increasing attention over the last decade. Several models based on simple/multi scaling and multifractal ideas have been put forth and parameter estimation techniques developed for the hypothesized models. Simulations based on these models have realistic resemblence to "generic rainfall fields". In this research we analyze rainfall data for scaling characteristics without an a priori assumed model. We look at the behavior of rainfall fluctuations obtained at several scales, via orthogonal wavelet transform of the data, to infer the precise nature of scaling exhibited by spatial rainfall. The essential idea behind the analysis is to segregate large scale (long wavelength) features from small scale features and study them independently of each other. The hypothesis is set forward that rainfall might exhibit scaling in small scale fluctuations, if at all, and at large scale this behavior will break down to accomodate the effects of external factors affecting the particular rain producing mechanism. The validity of this hypothesis is examined. In addition we define and estimate parameters that characterize the spatial dependence of the rainfall fluctuations and we use these parameters, estimated for several frames (in time), to relate to and identify the evolutionary nature of rainfall. These parameters and the type of scaling show significant variation from one rainfall field to another.

1. Introduction. A characteristic feature of precipitation is its extreme variability over time intervals of minutes to years and in space range of a few to thousands of square kilometers. One of the major challenges of hydrologists, meteorologists, and climatologists is to measure, model and predict the nature of this variability over different scales. Recent research (e.g. Lovejoy and Schertzer, 1990; Gupta and Waymire, 1990; and references therein) has indicated the exciting possibility that rainfall may exhibit scaling/multiscaling characteristics. The presence of such a hidden structure in the highly irregular patterns of rainfall at different spatial scales promises improved understanding of the precipitation process and new approaches to efficient modeling, measurement and prediction.

Early on, empirical study of contours of rain intensities (Lovejoy, 1982) and probability distribution functions of rain rates (Lovejoy and Mandelbrot, 1985) suggested scaling in rainfall. Later, it was argued by Kedem and Chiu (1987) that, since rainfall is an intermittent positive process giving rise to a mixed distribution with an "atom at zero", it could not be self-similar or simple scaling at least to the extent that a single parameter

* This research was supported by National Science Foundation grants BSC-8957469 and EAR-9117866 and by NASA under a graduate student fellowship for Global Change Research. We also thank the Minnesota Supercomputer Institute for providing us with supercomputer resources.

† Code 974, Bldg. 22, Rm. # G78, NASA-Goddard Space Flight Center, Greenbelt, MD 20771.

‡ St. Anthony Falls Hydraulic Laboratory, Department of Civil and Mineral Engineering, University of Minnesota, Minneapolis, MN 55414.

would not be sufficient to characterize this process. Lovejoy and Schertzer (1989) argued that although the rainfall intensities suffer this limitation, the rainfall fluctuations do not and could be modeled as self-similar process. They, however, did not empirically study the rainfall fluctuations for scaling characteristics but rather, using analogy from turbulence which is also an intermittent process, concentrated on further developing their multifractal models of rain (Lovejoy and Schertzer, 1987). Gupta and Waymire (1990) studied the moments of marginal distribution function of rainfall process conditioned on being positive and reported deviations from simple scaling. They proceeded with the development of a multiscaling theory of rain.

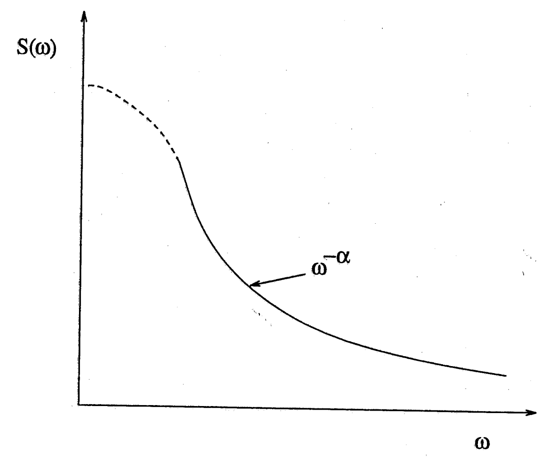

FIG. 1.1. *Schematic showing departure from power law at low frequencies in the spectrum of a physical process. The dotted line indicates the region of departure.*

In this research the hypothesis is set forward that rainfall can be decomposed in a large scale component representing the mean behavior of the process, and small scale fluctuations which exhibit self-similarity. The motivation for our hypothesis is based on physical arguments and empirical evidence. Theoretically, self-similarity implies infinite variance which results from the spectrum $S(\omega) \rightarrow \infty$ as $\omega \rightarrow 0$. This is physically unrealizable since all physical processes have finite energy. This results in the spectrum deviating from powerlaw behavior at very low frequencies (see Figure 1.1). Thus, in nature it is the fluctuations (deviations from a large scale mean component) that may exhibit self-similarity, if at all. In the context of rainfall, the very low frequencies in the spatial rain-intensity spectrum can be seen to be representing the morphological organization or the large scale forcing specific to that rain producing mechanism (for example effects of fronts in a squall line). When this effect is subtracted, the deviations which result from the local effects may obey some universality condition like self-similarity. It might also be that we can attribute low

frequency components to a deterministic process that should be eliminated before any stochastic consideration is taken into account. The spectrum of rain intensities do indeed show such regimes (see Figure 1.2). In all of the previous research, such a consideration of segregating large scale from small scale behavior, has not been taken into account for the purpose of analysis and inference of rainfall process. Our research is an effort towards this direction and develops a framework for segregating rainfall in large and small scale features and studying small scale features (fluctuations) for self-similarity.

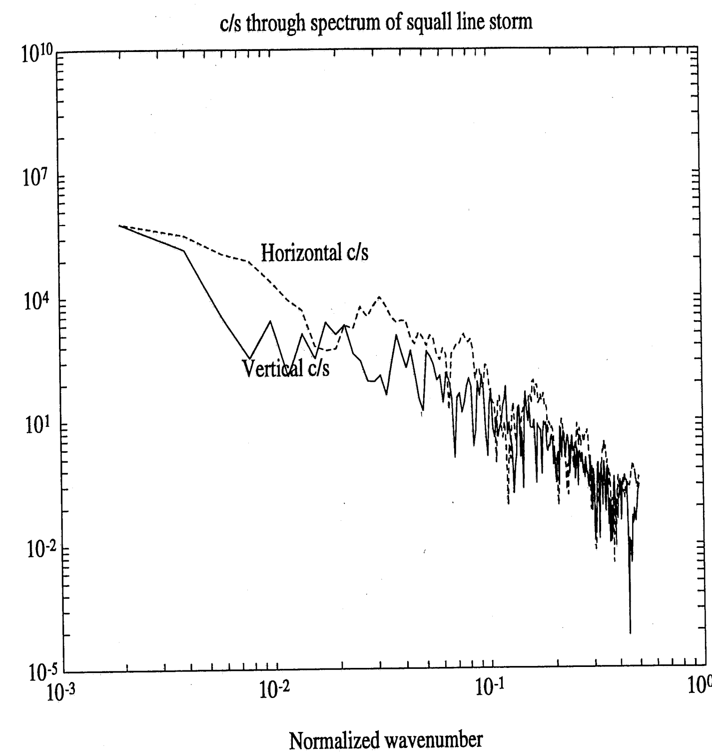

FIG. 1.2. *Horizontal and vertical cross sections through the two dimensional spectrum of a spatial rainfall field.*

The basic requirements from any methodology designed for such a purpose are: (i) data windowing capability so that non-homogeneities can be localized; (ii) adjustable window size so that no a priori information on the size of these features is required; and (iii) consistency across scales, i.e., features extracted at a certain scale directly from the data, or through an intermediate scale, should be the same. The methodology based on orthogonal wavelets discussed here elegantly embodies these requirements. The multiscale segregation achieved is such that statistics like the mean and correlation function of the component processes are additive. Also, the orthogonality of scale function and wavelets provide some additional optimality properties of multiscale discretization of the process or its fluctuations without any redundancy or loss of information. These properties are particularly attractive for the statistical analysis and inference of the rainfall process under study.

In addition to segregation of features of different scales, our research explicitly addresses the following issues which are other distinct advantages of the proposed method of analysis: (1) it can incorporate anisotropy and inhomogeneity and (ii) we study the evolutionary behavior of the storm. Our main interest is in analyzing and eventually modeling particular storms, e.g., a squall line or a convective storm, and not a "generic storm" derived from "averaging" over many realizations often obtained by invoking the assumption of stationarity over time and space. Thus, being able to account for anisotropy and non-homogeneity and identify how they characterize the features of the rainfall process at hand is an essential element of our analysis.

This paper is structured as follows. In section 2 we briefly review the theory of wavelet multiresolution framework. Section 3 describes an optimal multiscale discretization of stochastic processes which forms the basis on which the analysis and interpretation of rainfall data is based. Section 4 defines the notion of multicomponent scaling which is used for analyzing rainfall data. The details of analysis and results from applying the developed methodology to a squall line storm are described in section 5.

2. Wavelet multiresolution framework: review. Our methodology for analysis of rainfall fluctuations is based on wavelet multiresolution framework (see Mallat, 1989, and Daubechies, 1992). Wavelet multiresolution framework of the Hilbert space of square integrable functions $L^2(\mathbf{R})$ consists of a sequence of closed subspaces $\{V_m\}_{m\in\mathbf{Z}}$ of $L^2(\mathbf{R})$ ($\mathbf{Z}$ denotes the set of integers and $\mathbf{R}$ the real line) which satisfy the following properties:

- M1 $V_m \subset V_{m+1}$ $\forall m \in \mathbf{Z}$, i.e., a space corresponding to some resolution contains all the information about the space at lower resolution.
- M2 $\cup_{m=-\infty}^{\infty} V_m$ is dense in $L^2(\mathbf{R})$ and $\cap_{m=-\infty}^{\infty} V_m = \{0\}$, i.e., as the resolution increases the approximated function converges to the original function, and as the resolution decreases the approximated function contains less and less information.
- M3 $f(t) \in V_m$ iff $f(2t) \in V_{m+1}$ $\forall m \in \mathbf{Z}$, i.e., all spaces are scaled versions of one space. It is this property that leads to the multiresolution framework.
- M4 $f(t) \in V_m$ implies $f(t - \frac{k}{2^m}) \in V_m$ $\forall k \in \mathbf{Z}$, i.e., the space is invariant with respect to "integer translations" of a function.

In the interpretation of multiresolution framework, the projections of a function $f(t)$ on the subspaces V_m are viewed as successive approximations of $f(t)$ at finer and finer resolutions as m increases. The representation of functions in these subspaces V_m are obtained through an orthogonal projection by constructing an orthonormal basis for these subspaces. It is possible to construct a function $\phi(t)$ in V_0, called the **scale function**, satisfying $\int \phi(t)\,dt = 1$ and having compact support, such that $\{\phi(t-n)\}_{n\in\mathbf{Z}}$ is an orthonormal basis of V_0. Let O_0 be the orthogonal complement of V_0 in V_1, i.e.,

$$V_1 = V_0 \oplus O_0 \tag{2.1}$$

It is possible to construct a function $\psi(t)$, based on $\phi(t)$, such that $\{\psi(t-n)\}_{n\in\mathbf{Z}}$ is an orthonormal basis of O_0. The function $\phi(t)$ is orthogonal to its integer translates, and $\psi(t)$ is orthogonal to its integer translates and dyadic dilates. The function $\phi(t)$ is such that $\{2^{m/2}\phi(2^m t - n)\}_{n\in\mathbf{Z}}$ constitute an orthonormal basis of V_m. Using the recursive definition of equation (2.1) along with property M1 and the orthogonality of $\psi(t)$ with its integer translates and dyadic dilates, it can be shown that the dilates on the dyadic sequence and translates on integers of $\psi(t)$, i.e., $\{2^{m/2}\psi(2^m t - n)\}_{m,n\in\mathbf{Z}^2}$, form an orthonormal basis of $L^2(\mathbf{R})$. The function $\psi(t)$ is called an **orthogonal wavelet** and satisfies $\int \psi(t)\,dt = 0$ although higher order moments, i.e., $\int t^k \psi(t)\,dt$ for $k = 0, \ldots, N-1$, may also be zero.

The approximation of a function $f(t) \in L^2(\mathbf{R})$ at a resolution m, i.e., 2^m sample points per unit length, is given by the orthogonal projection of $f(t)$ on V_m. Let P_m represent this projection operator, i.e.,

$$f(t) \in L^2(\mathbf{R}) \Rightarrow P_m f(t) \in V_m \subset L^2(\mathbf{R}) \tag{2.2}$$

Using the basis functions $\phi(t)$ and $\psi(t)$ as described above, we can obtain

$$P_m f(t) = 2^{-m} \sum_{n=-\infty}^{\infty} (f, \phi_{mn}) \phi_{mn}(t) \tag{2.3}$$

where $\phi_{mn}(t) = 2^m \phi(2^m t - n)$ and (f, g) denotes the inner product in $L^2(\mathbf{R})$ defined for real functions as $\int_{-\infty}^{\infty} f(t)g(t)dt$. Let $Q_m f(t)$ represent the orthogonal projection of $f(t)$ onto O_m. Then we can obtain,

$$Q_m f(t) = 2^{-m} \sum_{n=-\infty}^{\infty} (f, \psi_{mn}) \psi_{mn}(t) \tag{2.4}$$

where $\psi_{mn}(t) = 2^m \psi(2^m t - n)$.

In multiresolution approximation, the values of the samples of the function at resolution m are exactly the inner products of $f(t)$ with the scale function $\phi_{mn}(t)$ for various values of n. The wavelet coefficients are used to express the additional details needed to go from one resolution to the next finer resolution level. Therefore, the set of inner products $P^d_m f = \{(f, \phi_{mn})\}_{n\in\mathbf{Z}}$ gives the discrete approximation of $f(t)$ (or sampled $f(t)$) at resolution m and the wavelet coefficients $Q^d_m f = \{(f, \psi_{mn})\}_{n\in\mathbf{Z}}$ give the discrete detail approximation of $f(t)$ (or difference in information between different resolutions). In other words we need to add the information contained in $Q^d_m f$ to $P^d_m f$ to go from resolution level m to the next higher resolution level $m+1$. For this reason, $Q_m f(t)$ is also referred to as the **detail function**.

For two dimensional multiresolution approximation we consider the function $f(t_1, t_2) \in L^2(\mathbf{R}^2)$. A multiresolution approximation of $L^2(\mathbf{R}^2)$ is a sequence of subspaces which satisfy the two dimensional extension of properties M1 through M5 enumerated above for the one dimensional multiresolution approximation. We again denote such a sequence of subspaces of $L^2(\mathbf{R}^2)$ by $(V_m)_{m\in\mathbf{Z}}$. The approximation of the function $f(t_1, t_2)$ at the resolution m, i.e., 2^{2m} samples per unit area, is the orthogonal projection on the vector space V_m.

A two dimensional multiresolution approximation is called separable if each vector space V_m can be decomposed as a tensor product of two identical subspaces V^1_m of $L^2(\mathbf{R})$, i.e., the representation is computed by filtering the signal with a low pass filter of the form $\Phi(t_1, t_2) = \phi(t_1)\phi(t_2)$. For a separable multiresolution approximation of $L^2(\mathbf{R}^2)$,

$$V_m = V^1_m \otimes V^1_m \tag{2.5}$$

where $\otimes$ represents a tensor product. It, therefore, follows (by expanding V_{m+1} as in 2.5 and using property M1) that the orthogonal complement O_m of V_m in V_{m+1} consists of the direct sum of three subspaces, i.e.,

$$O_m = (V^1_m \otimes O^1_m) \oplus (O^1_m \otimes V^1_m) \oplus (O^1_m \otimes O^1_m). \tag{2.6}$$

The orthonormal basis for V_m is then given by

$$\begin{aligned}&(2^{-m}\Phi_m(t_1 - 2^{-m}n, t_2 - 2^{-m}k))_{(n,k)\in\mathbf{Z}^2}\\ &\quad = (2^{-m}\phi_m(t_1 - 2^{-m}n)\phi_m(t_2 - 2^{-m}k))_{(n,k)\in\mathbf{Z}^2}.\end{aligned} \tag{2.7}$$

Analogous to the one dimensional case, the detail function at the resolution m is equal to the orthogonal projection of the function on to the space O_m which is the orthogonal complement of V_m in V_{m+1}. An orthonormal basis for O_m can be built based on Theorem 4 in Mallat (1989, pg. 683) who shows that if $\psi(t_1)$ is the one dimensional wavelet associated with the scaling function $\phi(t_1)$, then, the three "wavelets" $\Psi^1(t_1, t_2) = \phi(t_1)\psi(t_2)$ $\Psi^2(t_1, t_2) = \psi(t_1)\phi(t_2)$ and $\Psi^3(t_1, t_2) = \psi(t_1)\psi(t_2)$ are such that

$$\{(\Psi^1_{mnk}, \Psi^2_{mnk}, \Psi^3_{mnk})_{(n,k)\in\mathbf{Z}^2}\}$$

is an orthonormal basis for O_m and

$$\{(\Psi^1_{mnk}, \Psi^2_{mnk}, \Psi^3_{mnk})_{(m,n,k)\in\mathbf{Z}^3}\}$$

is an orthonormal basis of $L^2(\mathbf{R}^2)$, where $\Psi^i_{mnk} = 2^{-m}\Psi^i_m(t_1 - 2^{-m}n, t_2 - 2^{-m}k)$

The discrete approximation of the function $f(t_1, t_2)$ at a resolution m is obtained through the inner products

$$P^d_m f = \{(f, \Phi_{mnk})_{(n,k)\in\mathbf{Z}^2}\} = \{(f, \phi_{mn}\phi_{mk})_{(n,k)\in\mathbf{Z}^2}\} \tag{2.8}$$

The discrete detail approximation of the function is obtained by the inner product of $f(t_1, t_2)$ with each of the vectors of the orthonormal basis of O_m. This is thus given by

$$\begin{aligned}Q^{d^1}_m f &= \{(f, \Psi^1_{mnk})_{(n,k)\in\mathbf{Z}^2}\},\\ Q^{d^2}_m f &= \{(f, \Psi^2_{mnk})_{(n,k)\in\mathbf{Z}^2}\},\\ Q^{d^3}_m f &= \{(f, \Psi^3_{mnk})_{(n,k)\in\mathbf{Z}^2}\}.\end{aligned} \tag{2.9}$$

The corresponding continuous approximation will be denoted by $Q^1_m f(t)$, $Q^2_m f(t)$ and $Q^3_m f(t)$, respectively. For the implementation to discrete data see Mallat (1989).

The decomposition of O_m into the sum of three subspaces (see equation (2.6)) gives the behavior of spatially oriented frequency channels. Assume that we have a discrete process at some resolution $m+1$ whose frequency domain is shown in Figure 2.1 as the domain of $P^d_{m+1} f$. When the same process is reduced to resolution m, its frequency domain shrinks to that of $P^d_m f$. The information lost can be divided into three components as shown in Figure 2.1: vertical high frequencies (high horizontal correlation), horizontal high frequencies (high vertical correlation) and high frequencies in both direction (high vertical and horizontal correlations, for example, features like corners). These components are captured as $Q^{d^1}_m f$, $Q^{d^2}_m f$ and $Q^{d^3}_m f$ respectively. We will use this property to characterize the directional behavior of rainfall.

3. Multiscale discretization of mean and fluctuations of a stochastic process. We now argue that the inner product of a stochastic process with scale functions and wavelets may be regarded as optimal discretizations (in a sense described below) of mean and fluctuations of the process. From the theory of multiresolution decomposition it can be seen that, for a stochastic process $X(t)$, the discrete values $\{(X, \phi_{mn})\}_{n\in\mathbf{Z}}$ obtained as $(X, \phi_{mn}) = \int X(t)\phi_{mn}(t)\,dt$ constitute an optimal discretization of $X(t)$ at the resolution m in the least squares sense if the realization of $X(t)$ is regarded as a function in $L^2(\mathbf{R})$. However, in a probabilistic framework, the multiresolution framework provides additional, significant, non-trivial extensions as can be seen from the following three properties.

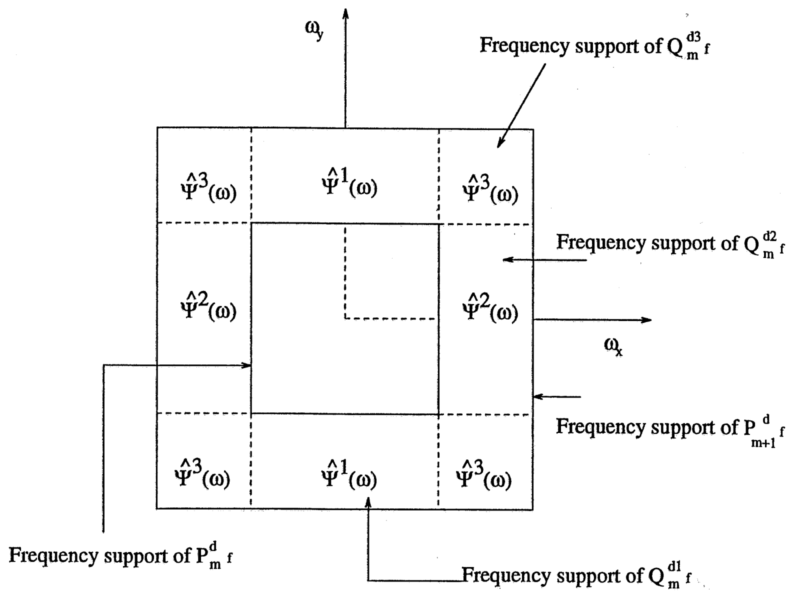

FIG. 2.1. *Frequency support of wavelets in two dimensional multiresolution decomposition.*

P1 There is no redundancy in the discretization at any resolution since the integration kernels are linearly independent of their translates, or in other words the finite dimensional joint distribution function of the random variables $\underline{X} = \{(X, \phi_{mn_1}), \ldots, (X, \phi_{mn_\nu})\}$ is non-degenerate. That is, there exists no subspace of dimension $\nu' < \nu$ such that $\int_{\mathbf{R}^{\nu'}} p_m(\underline{x}')\, d\underline{x}' = \int_{\mathbf{R}^{\nu}} p_m(\underline{x})\, d\underline{x}$, where $\underline{x}' \in \mathbf{R}^{\nu'}$, $\underline{x} \in \mathbf{R}^{\nu}$.

P2 The discretization at any resolution m is "maximal" as the translates of the integration kernel span the complete space V_m, i.e., the joint distribution function of any finite subset of random variables from the *infinite* set $\{X_n = (X, \phi_{mn})\}_{n \in \mathbf{Z}}$ of random variables is unique.

P3 The above properties hold for all dyadic scales (resolutions), thus providing elegant discretizations at a hierarchy of scales. This property makes multiresolution framework very attractive for multiscale studies.

Since ϕ_{mn} is an averaging function, by virtue of the above properties, the inner products of the process with the scale functions may be regarded as the discretizations of the mean process at the scale 2^{-m}

While the representation of the process from one resolution to a lower one is obtained via the scale function, the information lost during this transformation is preserved as the sequence (wavelet coefficients) $Q_m^d X \equiv$

$\{(X, \psi_{mn})\}_{n \in \mathbf{Z}}$, or equivalently the detail function $Q_m X(t)$. Alternatively, these coefficients can be also viewed as discretization of fluctuations of $X(t)$. By choosing the wavelet $\psi_{mn}(t)$ as the integration kernel we see that the discretization we obtain is optimal in the same sense as discussed above but with the space under consideration being O_m. The wavelet coefficients can be regarded as discretization of the fluctuations of $X(t)$ in the sense that these values give the deviation of the process from its local mean. If $X(t)$ is a process with stationary increments of order N, then by choosing an orthogonal wavelet with N vanishing moments, denoted as ${}_N\psi_{mn}$ (using the terminology of Daubechies (1988)), we obtain a stationary sequence of wavelet coefficients $Q_m^d X = \{(X, {}_N\psi_{mn})\}$ (see Kumar and Foufoula-Georgiou, (1992a)). This sequence, therefore, represents an optimal discretization of the fluctuations of $X(t)$ at the scale 2^{-m}. Thus, wavelet transforms provide a way to study non-stationary stochastic processes. In addition, the above results are valid for all dyadic scales 2^{-m} $(m \in \mathbf{Z})$ which makes wavelets attractive for *multiscale study* of non-homogeneous processes.

4. Multicomponent self-similarity. In general a non-homogeneous process can be made tractable by decomposing it into simpler component processes in a variety of ways (see Vanmarcke 1983, pg. 224). We choose to decompose the process into mean and fluctuations, i.e., $X(\mathbf{t}) = \overline{X}(\mathbf{t}) + X'(\mathbf{t})$, for its physical significance of capturing large and small scale behavior of the process. We approximate the mean, $\overline{X}(\mathbf{t})$, and fluctuations, $X'(\mathbf{t})$, at some resolution m_0 using scale functions and wavelets as $\overline{X}(\mathbf{t}) \approx \overline{X}_{m_0}(\mathbf{t})$ and $X'(\mathbf{t}) = \sum_{m > m_0} X'_m(\mathbf{t})$ where

$$\overline{X}_m(\mathbf{t}) = \sum_{n,k} (X, \Phi_{mnk}) \Phi_{mnk}(\mathbf{t}) \tag{4.1}$$

and the fluctuation field at resolution m is composed of three components

$$X'_m(\mathbf{t}) = \sum_{n,k} (X, \Psi^1_{mnk}) \Psi^1_{mnk}(\mathbf{t}) + \sum_{n,k} (X, \Psi^2_{mnk}) \Psi^2_{mnk}(\mathbf{t}) + \sum_{n,k} (X, \Psi^3_{mnk}) \Psi^3_{mnk}(\mathbf{t}) \tag{4.2}$$

$$\equiv X'_{1,m}(\mathbf{t}) + X'_{2,m}(\mathbf{t}) + X'_{3,m}(\mathbf{t}). \tag{4.3}$$

where $X'_{i,m}(\mathbf{t})$ is used to denote the component $\{Q^i_m X(t)\}$ of the wavelet decomposition. Therefore,

$$X'(\mathbf{t}) = \sum_{m \geq m_0} (X'_{1,m}(\mathbf{t}) + X'_{2,m}(\mathbf{t}) + X'_{3,m}(\mathbf{t})) \tag{4.4}$$

$$\equiv X'_1(\mathbf{t}) + X'_2(\mathbf{t}) + X'_3(\mathbf{t}). \tag{4.5}$$

The scale 2^{-m_0} (or resolution m_0) will be determined from physical considerations, as the largest scale upto which rainfall fluctuations exhibit self-similarity.

The advantages of the above approximation are enumerated below.

1. The mean field $\overline{X}_m(\mathbf{t})$ represents the large scale behavior of the process. No assumption about the homogeneity of the mean field is required since the representation (4.1) is constructed using transformation that is local.
2. The fluctuation field at some resolution m, $X'_m(t)$, itself consists of three components giving the directional information about the storm. We will assume that each of these three fields are homogeneous. Since the fluctuation components are extracted using independent spatially oriented frequency channels they are uncorrelated (see Yaglom, 1987, eq. 2.205) and the covariance $R'_m(\mathbf{t},\mathbf{s})$ of $X'_m(\mathbf{t})$ itself can be written as the sum of the covariances of these three components, i.e.,

$$R'_m(\mathbf{t},\mathbf{s}) = R'_{1,m}(\mathbf{t},\mathbf{s}) + R'_{2,m}(\mathbf{t},\mathbf{s}) + R'_{3,m}(\mathbf{t},\mathbf{s}) \tag{4.6}$$

and

$$R'(\mathbf{t},\mathbf{s}) = \sum_{m\geq m_0} (R'_{1,m}(\mathbf{t},\mathbf{s}) + R'_{2,m}(\mathbf{t},\mathbf{s}) + R'_{3,m}(\mathbf{t},\mathbf{s})) \tag{4.7}$$

$$\equiv R'_1(\mathbf{t},\mathbf{s}) + R'_2(\mathbf{t},\mathbf{s}) + R'_3(\mathbf{t},\mathbf{s}) \tag{4.8}$$

We conjecture that the external factors governing the storm mostly influence the large scale behavior (or the mean field) and the small scale behavior (or fluctuation field) is relatively independent of this influence. We hypothesise that $X'(\mathbf{t})$ may be scaling in the sense that

$$\{X'_1(\lambda\mathbf{t})\} \stackrel{d}{=} \{\lambda^{H_1} X'_1(\mathbf{t})\}, \tag{4.9}$$

$$\{X'_2(\lambda\mathbf{t})\} \stackrel{d}{=} \{\lambda^{H_2} X'_2(\mathbf{t})\}, \tag{4.10}$$

$$\{X'_3(\lambda\mathbf{t})\} \stackrel{d}{=} \{\lambda^{H_3} X'_3(\mathbf{t})\}. \tag{4.11}$$

where the above equalities are in terms of the **joint distribution of the discretizations** of the corresponding fluctuation processes. The scaling exponents H_1, H_2, and H_3 need not be the same. We regard $X'_{d1,m}$ as the discretization of X'_1 at various resolutions m (or equivalently at different scales 2^{-m}) and analogously for the other components $X'_{d2,m}$ and $X'_{d3,m}$. We call such a scaling behavior as **multicomponent scaling**. We perform multiscale analysis on each of these components to establish the precise nature of their scaling properties.

5. Application to rainfall fields. Mathematically self-similar processes are defined as processes whose finite dimensional joint distribution function satisfies equation (see Lamperti, 1962)

$$\begin{aligned} Pr(\lambda^{-H}X(\lambda t_1) < x_1, \ldots, \lambda^{-H}X(\lambda t_n) < x_n) \\ = Pr(X(t_1) < x_1, \ldots, X(t_n) < x_n). \end{aligned} \tag{5.1}$$

which is also written as

$$\{X(\lambda t)\} \stackrel{d}{=} \{\lambda^H X(t)\} \qquad H \in \mathbf{R},\ \lambda \in \mathbf{R}^+ \tag{5.2}$$

By nature of the transformation involved, the n dimensional multivariate joint probability distribution function, $p(\underline{x};\underline{t})$, $\underline{x},\underline{t} \in \mathbf{R}^n$, of the random vector $\underline{X} = \{X(t_1), \cdots, X(t_n)\}$, necessarily satisfies

$$p(\underline{x};\underline{t}) = \lambda^H p(\lambda^H \underline{x}; \lambda\underline{t}) \tag{5.3}$$

The marginal distribution function satisfies

$$p(x;t) = \lambda^H p(\lambda^H x; \lambda t). \tag{5.4}$$

The notation $p(\underline{x};\underline{t})$ indicates that the distribution function of $\underline{X}$ is specified by parameters that depend on $\underline{t}$. The above condition (5.3) can be translated into a requirement for the characteristic function of the multidimensional distribution, $\rho(\underline{\xi};\underline{t})$ as

$$\rho(\underline{\xi};\underline{t}) = \rho(\lambda^{-H}\underline{\xi}; \lambda\underline{t}) \tag{5.5}$$

or, equivalently for the characteristic function of the marginal distribution

$$\rho(\xi;t) = \rho(\lambda^{-H}\xi; \lambda t). \tag{5.6}$$

In general, the probability distributions $p(\underline{x};\underline{t})$ satisfying (5.3) are described by stable distributions, Gaussian being the limiting case of these distributions having finite variance. The rainfall fluctuations are found to have a symmetric distribution and hence we will be concerned with symmetric stable distributions. In general, the marginal characteristic function of a symmetric stable distribution is given by (see Stuart and Ord, 1987)

$$\rho(\xi;t) = \exp(-|c(t)\xi|^\alpha) \tag{5.7}$$

where α is called the characteristic exponent and c as the scale parameter. For it to be self-similar, i.e., satisfy equation (5.5), we need to have

$$c(\lambda t) = \lambda^H c(t) \tag{5.8}$$

or equivalently

$$\log c(\lambda) = H \log \lambda + \log c(1). \tag{5.9}$$

For estimation of the parameters α and c at any given scale λ see Kumar and Foufoula-Georgiou (1992b).

To find if the fluctuations of the rainfall process scale in the sense of equation (4.9-4.11) we study the marginal distribution function of the discretizations of the component processes $\{X'_{di,m}\}_{i=1,2,3}$ at different scales 2^{-m}. The data used is a severe squall line storm which occurred over Norman, Oklahoma on May 27, 1987. The rainfall intensity values at ground level for this storm are available at temporal integration scale of 10 minutes (for a period of 7 hours beginning with the mature stage of the core of the squall line), for 360 azimuths, with every azimuth containing 115 estimates for a range of 230 kilometers (i.e., data at every 2 km by 1 degree). The steps involved in the analysis are summarized below:

1. Check if the discretizations of rainfall fluctuations $X'_{di,m}$ at each resolution m obey a stable law or can be approximated by one, i.e., estimate parameters α and c. Table 5.1 gives the estimates of α and c for each of the three components at various resolutions for the first frame of the dataset.
2. Check the goodness of fit of the stable distribution. Having estimated the parameters of the stable distribution, the theoretical and empirical cdf is plotted for each component at each scale to test the goodness of fit. (See Figure 5.1 for such a fit at one resolution; fit at other resolutions are similar.) The empirical cdf was obtained using Weibull plotting positions. The theoretical cdfs for various α and c values were estimated by the methodology described in Holt and Crow (1973).
3. If the rainfall fluctuations can be described by a stable law, test to see if they exhibit scaling, i.e., satisfy equation (5.9). If the rainfall fluctuations are not self-similar at all scales, determine the critical resolution m_0 up to which scaling is observed and estimate H using equation 5.9 (see Figure 5.2). The resolution m_0 is determined from the point of departure from linearity in the log-log plot of the scale parameter c with scale λ. The point of departure is found to correspond to a scale of approximately 30 × 30 km and this result is consistent across several frames. The slope of the graph up to scale 2^{-m_0} gives the estimate of the parameter H (see Table 5.1).
4. Study the evolutionary behavior of the storm by studying the changes in $\{\alpha_i\}_{i=1,2,3}$ and $\{H_i\}_{i=1,3}$ across frames. Under our hypothesis the characteristic exponent $\{\alpha_i\}$ for the marginal distribution of $\{X'_{di,m}\}_{i=1,2,3}$ is expected to be the same for all resolutions m. However, variations were observed in the estimated values of α. To study the evolutionary structure of the storm, $\overline{\alpha_i}$ and H_i were plotted for various frames for all datasets (see Figure 5.3). The results for the 10 frames shown in the figure are at every 10 minutes starting from the peak of the core of the storm, i.e., they correspond to the dissipative phase of the core. As is evident from the figure, low α values (or large fluctuations) are observed when the core is still intense, and the α values decrease as the storm dissipates. The nature of dependence as indicated by H is very persistent across several frames.

The results of this study indicate that multicomponent self-similar models are viable models for describing the behavior of rainfall fluctuations for scales upto 30 kms. Alternate identification techniques using probability weighted moments have also corroborated this conclusion (see Kumar et al., 1992).

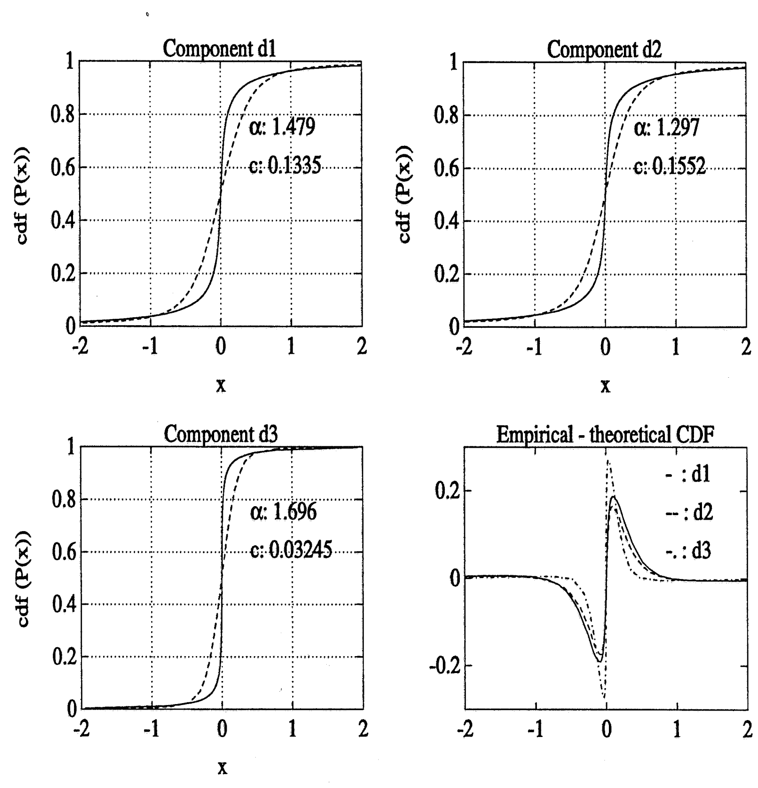

FIG. 5.1. *Empirical (solid lines) and theoretical (dotted lines) cumulative distribution functions for the three components d1, d2 and d3 of frame 1 the squall line storm. The figure also shows the difference between the empirical and theoretical cumulative distribution functions for all components.*

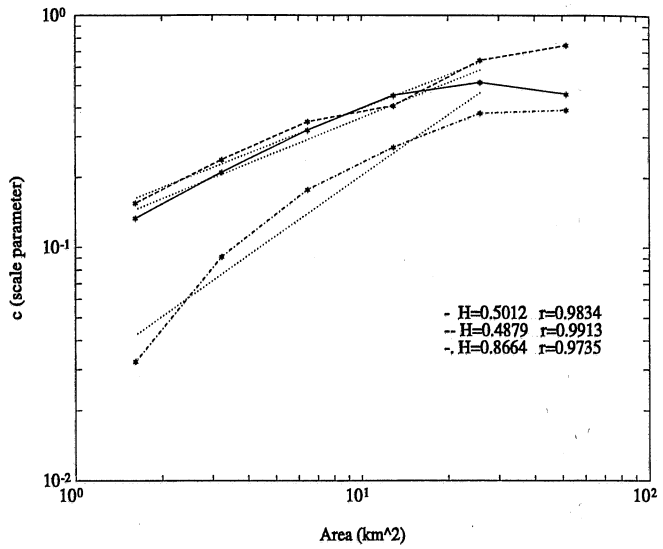

FIG. 5.2. *Log-log plot of scale parameter with respect to scale for frame 1 of the squall line storm. The solid line is for component d1, dotted line for d2, and dot-dashed line for d3. The regression lines obtained using five levels of decomposition are also indicated in the figure.*

TABLE 5.1

Estimates of α and c for the squall line storm at various levels of decomposition. The table also gives the mean $\overline{\alpha}$ and H estimated using the first five levels of decomposition. The correlation coefficient, r, for the estimation of H is also indicated.

		Frame 1 (11:52am to 12:02pm)				
component	Grid	α	c	$\overline{\alpha}$	H	r
$d1$	256 × 256	1.479	0.134			
	128 × 128	1.376	0.211			
	64 × 64	1.378	0.320			
	32 × 32	1.561	0.454			
	16 × 16	1.620	0.516	1.483	0.501	0.983
	8 × 8	1.981	0.460			
$d2$	256 × 256	1.297	0.155			
	128 × 128	1.189	0.238			
	64 × 64	1.062	0.348			
	32 × 32	1.048	0.409			
	16 × 16	1.514	0.643	1.222	0.488	0.991
	8 × 8	1.480	0.746			
$d3$	256 × 256	1.696	0.032			
	128 × 128	1.668	0.091			
	64 × 64	1.546	0.178			
	32 × 32	1.456	0.270			
	16 × 16	1.506	0.380	1.575	0.866	0.974
	8 × 8	1.892	0.393			

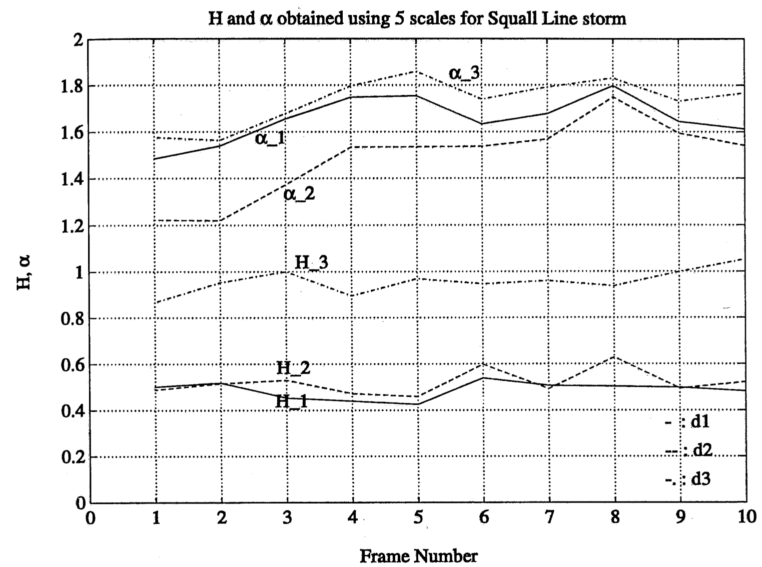

FIG. 5.3. *Time evolution of $\overline{\alpha_i}$ and H_i.*

REFERENCES

[1] I. Daubechies, *Orthonormal bases of compactly supported wavelets*, Commun. on Pure and Appl. Math., Vol. XLI, (1988), pp. 901–996.

[2] I. Daubechies, *Ten Lectures on Wavelets*, SIAM, Philadelphia, 1992.

[3] V. Gupta and E. Waymire, Multiscaling properties of spatial rainfall and river flow distributions, J. Geophys. Res., 95(D3), (1990), pp. 1999–2009.

[4] D.R. Holt and E.L. Crow, *Tables and graphs of stable probability density functions*, J. of Res. of the National Bureau of Std.—B. Math. Sci., 77B(3 and 4), July-Dec (1973), pp. 143–198.

[5] B. Kedem and L.S. Chiu, *Are rain rate processes self-similar?*, Water Resour. Res., 23(10), (1987), pp. 1816–1818.

[6] P. Kumar and E. Foufoula-Georgiou, *A multicomponent decomposition of spatial rainfall fields: 1. segregation of large and small scale features using wavelet transforms*, Water Resour. Res., (under review) (1992a).

[7] P. Kumar and E. Foufoula-Georgiou, *A multicomponent decomposition of spatial rainfall fields: 2. self-similarity in fluctuations*, Water Resour. Res., (under review) (1992b).

[8] P. Kumar, P. Guttorp and E. Foufoula-Georgiou, *A probability weighted moment test for scaling and application to assessing scaling in rainfall fields*, Water Resour. Res., (under preparation) (1992).

[9] J. Lamperti, *Semi-stable stochastic processes*, Trans. Amer. Math. Soc., 104, (1962), pp. 62–78.

[10] S. Lovejoy, *The area perimeter relation for rain and cloud*, Science, 216, (1982), pp. 185–187.

[11] S. Lovejoy and B.B. Mandelbrot, *Fractal properties of rain and a fractal model*, Tellus, 37A, (1985), pp. 209–232.

[12] S. Lovejoy and D. Schertzer, *Physical modeling and analysis of rain and clouds by anisotropic scaling multiplicative processes*, J. Geophys. Res., 92(D8), (1987), pp. 9693–9714.

[13] S. Lovejoy and D. Schertzer, *Comment on "Are Rain Rate Processes Self-Similar?"*, Water Resouces Res., Vol. 25, No. 13, March (1989), pp. 577–579.

[14] S. Lovejoy and D. Schertzer, *Multifractals, universality classes and satellite and radar measurements of cloud and rain fields*, J. Geophys. Res., 95 (D3), (1990), pp. 2021–2034.

[15] S. Mallat, *A theory for multiresolution signal decomposition: the wavelet representation*, IEEE Tran. on Pattern Anal. and Mach. Intel., 11(7), (1989), pp. 674–693.

[16] A. Stuart and J.K. Ord, *Kendall's Advanced Theory of Statistics Vol. 1*, Oxford University Press, New York, 1987.

[17] E. Vanmarcke, *Random Fields: Analysis and Synthesis*, The MIT Press, Cambridge, Massachusetts, 1983.

[18] A.M. Yaglom, *Correlation Theory of Stationary and Related Random Functions, I: Basic Results*, Springer-Verlag, New York, 1987.

ESTIMATION OF KINETIC RATE COEFFICIENTS FOR 2,4-D BIODEGRADATION DURING TRANSPORT IN SOIL COLUMNS

R.S. MAIER*, W.J. MAIER†, B. MOHAMMADI‡, R. ESTRELLA§, M.L. BRUSSEAU§, AND R.M. MILLER§

Abstract. The Monod model is used increasingly to simulate the kinetics of biodegradation in soil environments with distinctly different hydraulic properties than the well-mixed batch reactor environments for which the model is known to be appropriate [17,19,20]. This paper investigates the use of a transport model with Monod kinetics to describe the fate of 2,4-D in soil columns. The research includes development of a mathematical model for the biodegradation of 2,4-D in the presence of an acclimated biological population and an optimization model to calibrate results of the mathematical model with experimental observations. The model is applied to experimental data from two independent soil column experiments to qualify the generality of the numerical results. Fitted kinetic parameters are compared with well-mixed batch reactor test data and goodness of fit is compared with a linear model of transport with first-order substrate decay. The fitted model is used to discuss strategies to minimize transport of 2,4-D into lower soil horizons and groundwater.

1. Introduction. Groundwater pollution is a potential result of pesticide usage. A potential mitigating factor is that soils may contain microorganism populations capable of biodegrading particular pesticides. The purpose of this paper is to examine the particular case of 2,4-dichlorophenoxyacetate (2,4-D), a widely-used herbicide known to be biodegradable, and to obtain quantitative descriptions of the potential for biodegradation in soil environments.

The natural purification capacity of soils is driven by the accumulation of natural organic matter and associated microbes that flourish in the upper soil horizons. The lower horizon soils typically have progressively lower organic contents and very low microbial populations. It is conjectured that 2,4-D removal requires biodegradation in the upper horizons otherwise it will percolate downward into the groundwater. An important question is whether and under what conditions microbial degradation can be relied on to remove 2,4-D and prevent groundwater pollution. A related question is whether removal is complete or whether potentially toxic intermediate products are transported into groundwater.

Aerobic biodegradation of 2,4-D has been observed for a variety of pure and mixed bacterial cultures derived from soils. Metabolic pathways

---

* Army High Performance Computing Research Center, University of Minnesota, 1100 Washington Ave. South, Minneapolis, MN 55415.

Work supported by Army Research Office contract number DAALO3-89-C-0038.

† Department of Civil and Mineral Engineering, University of Minnesota, Minneapolis, MN 55455.

‡ INRIA-MENUSIN, Domaine de Voluceau, BP. 105, 78153 Le Chesnay, France.

§ Department of Soil and Water Science, University of Arizona, Tucson, AZ 85721.